Pergamon

Int. J. Heat Mass Transfer. Vol. 41, No. 14, pp. 2083–2096, 1998

Printed in Great Britain
0017-9310/98 $19.00+0.00

PII: S0017-9310(97)00373-6

Transient conductive–radiative cooling of an optical quality glass disk

KONG HOON LEE† and RAYMOND VISKANTA‡

School of Mechanical Engineering, Purdue University, West Lafayette, IN 47907-1288, U.S.A.

(*Received* 26 *March* 1997 *and in final form* 20 *November* 1997)

Abstract—Transient combined conductive–radiative heat transfer is analyzed in an optical quality glass disk. Typically semitransparent materials such as a glass have spectrally selective absorption and emission characteristics. In the present analysis the spectral dependence of the absorption coefficient on wavelength is appropriately accounted for, and discrete ordinates method is used to solve the radiative transfer equation for the axisymmetric cylindrical geometry. Specularly reflecting boundaries are considered, and Fresnel's equations are used to predict the spectral radiation characteristics at the interfaces. The numerical analysis is validated by comparing predictions to the experimental results for soda-lime glass. As an example, BK7 optical quality glass is considered as a semitransparent medium. © 1998 Elsevier Science Ltd. All rights reserved.

INTRODUCTION

Accurate prediction of temperature distributions in glass and other semitransparent materials at high temperature are essential during various fabricating operations. For example, the annealing of glass plates requires prediction of the temperature distribution from the transient combined conduction and radiation heat transfer analysis. During the process of annealing optical quality glass which is utilized for optical components in imaging systems, the temperature gradients in the glass must be controlled very carefully by imposing a constant cooling rate of the order of 0.01°C/h, because a true geometric and color image of an object is generated by using the property of refraction. Even small stresses due to the temperature gradients in the annealing range cause permanent strains and inhomogeneities of the refractive index [1]. This can be detrimental to optical glasses of high quality. Moreover, the stress–strain relation in glass plate during annealing or tempering and danger of fracture is also strongly related to the temperature gradients [2]. Therefore, it is very important to preserve the uniform temperature distribution during the cooling of high quality optical glass. Thus, to insure the uniformity of temperature in glass, it is necessary to cool the glass at a very slow rate by varying the surrounding and/or ambient temperature with time.

In order to accurately predict the temperature distribution in the semitransparent materials such as glass at high temperature, the radiant energy transfer throughout the interior of the medium as well as the heat transfer by conduction needs to be considered. Conduction is the diffusive transfer of energy at the molecular (phonon) level, while radiation is the transport of energy by electromagnetic waves (photons) over a finite distance. In opaque materials, thermal energy is transferred only by conduction throughout the interior; however, in semitransparent materials, energy is transferred by simultaneous conduction and radiation, because the semitransparent nature of the material makes internal radiative transfer a very important component of overall heat transfer. Therefore, the local temperature and the local temperature gradients cannot be predicted accurately using the concept of the effective (apparent) thermal conductivity, and rigorous treatment of radiative transfer is needed [3, 4]. Typically, semitransparent materials such as glass are homogeneous and the scattering of radiation can be neglected in comparison to absorption, and this makes it easier to carry out the analysis of radiative heat transfer [5]. However, since semitransparent materials have the spectral absorption and refraction characteristics which depend strongly on wavelength and specularly reflecting boundaries, it is difficult to solve the radiative transfer equation analytically.

Much research has been directed towards the combined effects of conduction and radiation in glass. A pioneering transient analysis by Gardon [6] was on the heat treatment of glass plate. Specular boundary reflections were considered, and two spectral bands were used in the semitransparent spectral region with the glass assumed to be opaque for wavelengths larger than 4 μm. More recently, Ping and Lallemand [7] studied heat transfer in glass plates for several thermal and radiative boundary conditions using a nodal analysis based on the zonal method. The effects of many dimensionless parameters were investigated,

† Permantly at Advanced Institute of Machinery and Design, Seoul National University, Seoul 151-742, Korea.

‡ Author to whom correspondence should be addressed.

NOMENCLATURE

c	specific heat [J kg^{-1} K^{-1}]
$F_{z,\mathrm{op}}$	radiative flux defined by $F_{z,\mathrm{op}} = \int_{\lambda_c}^{\infty} F_{z,\lambda}\,\mathrm{d}\lambda$ [W m^{-2}]
$F_{z,\mathrm{sem}}$	radiative flux defined by $F_{z,\mathrm{sem}} = \int_{0}^{\lambda_c} F_{z,\lambda}\,\mathrm{d}\lambda$ [W m^{-2}]
$\mathbf{F}$	radiative heat flux vector [W m^{-2}]
g	fractional blackbody function defined by equation (7)
G	incident radiation flux [W m^{-2}]
h	convective heat transfer coefficient [W m^{-2} K^{-1})]
I	radiative intensity [W m^{-2} sr^{-1}]
I_b	blackbody intensity [W m^{-2} sr^{-1}]
k	thermal conductivity [W m^{-1} K^{-1}]
L	thickness of the glass disk [m]
n	coordinate normal to the surface
$\mathbf{n}$	unit vector normal to the surface
n_λ	refractive index
$\mathbf{q}$	conductive heat flux vector [W m^{-2}]
r	radial coordinate [m]
$\mathbf{r}$	spatial position vector [m]
R	radius of the glass disk [m]
t	time [s]
T	temperature [K or °C]
T_0	initial temperature [K or °C]
z	axial coordinate [m].

Greek symbols

ε	emissivity in the opaque spectral region
θ	polar angle, or angle defined as $\theta = \cos^{-1}(\mathbf{\Omega}\cdot\mathbf{n})$
κ_λ	spectral absorption coefficient [cm^{-1}]
λ	wavelength [m]
λ_c	cut-off wavelength [m]
μ, η, ξ	direction cosines defined by equation (10)
ρ	density [kg m^{-3}]
ρ_λ	reflectivity
ϕ	azimuthal angle
Ω	solid angle [sr]
$\mathbf{\Omega}$	unit vector into the direction of intensity.

Subscripts

∞	refers to ambient
b	refers to blackbody value
c	refers to center
op	refers to opaque spectral region
s	refers to surface
sem	refers to semitransparent spectral region
sur	refers to surrounding
λ	refers to wavelength or per unit wavelength.

Superscripts

m, l	discrete directions of intensity.

and internal radiation was found to have a very substantial effect on the uniformity of the transient temperature distributions. Su and Sutton [8] predicted temperatures and heat fluxes with 16 spectral bands in the silicate glass plate externally heated by a constant heat input at one boundary for a time interval of 5 s. The model considered specularly reflecting surfaces with characteristics described by the Fresnel's equation. The refractive index was considered to be a function of wavelength and temperature, and the glass was assumed opaque for wavelengths larger than 4 μm. The effect of variable refractive index on heat transfer was found to be small. Field and Viskanta [3] are the only investigators who have studied both experimentally and theoretically transient cooling of soda-lime glass plate. The plate was initially heated to a temperature near its softening point (approximately 550°C) then it was suddenly exposed to the cooling by free convection and radiation to the ambient surroundings. Internal radiation effects were found to be very significant as predicted by calculations. Five bands were considered in the semitransparent wavelength range (0–5 μm) and the glass was assumed to be opaque at larger wavelengths.

In this paper, an analysis is reported of transient cooling of a two-dimensional, axisymmetric optical quality glass disk by combined conduction and radiation. The problem is of both theoretical and technological interest in the manufacture of optical imaging components, and to the authors' knowledge has not been analyzed. The glass is considered a semitransparent medium capable of absorbing and emitting radiation, and the dependence of the adsorption coefficient on wavelength has been considered. As a specific example, the analysis simulates the annealing of a BK7 optical quality glass disk. The finite volume method is used to solve the thermal energy equation, and the discrete ordinates method (DOM, S–N method) is used to solve the radiative transfer equation (RTE). The numerical analysis has been carried out for an axisymmetric cylindrical medium and is validated by comparing the predictions with the avail-

able experimental data for cooling of a glass plate [3].

ANALYSIS

Model equation of transient conductive–radiative cooling

Consider the energy transport within a cylindrical semitransparent medium shown in Fig. 1. The medium is surrounded by isothermal black walls, and the space between the medium and the surrounding wall is either a vacuum ($n'_\lambda = 1$) or is occupied by a transparent entity having the refractive index of unity. In addition, the following assumptions are made in analysis: (1) the disk is axisymmetric, and heat transfer by conduction and radiation occurs axisymmetrically; (2) the medium emits and adsorbs but does not scatter thermal radiation; (3) the medium is in local thermodynamic equilibrium for which Planck's and Kirchhoff's laws are valid; (4) the spatial dimensions of the medium are much longer than the wavelength of radiation for the semitransparent band, i.e., the coherence effects are negligible; (5) the refractive index of the medium does not depend on temperature in the considered range; (6) the interface between the medium and the bounding entity is optically smooth; and (7) the surrounding walls are gray diffuse emitters of radiation.

Employing assumption (1), the transient two-dimensional axisymmetric energy equation is

$$\rho c\frac{\partial T}{\partial t} = -\nabla\cdot(\mathbf{q}+\mathbf{F}) = \frac{1}{r}\frac{\partial}{\partial r}\left(rk\frac{\partial T}{\partial r}\right) + \frac{\partial}{\partial z}\left(k\frac{\partial T}{\partial z}\right) - \nabla\cdot\mathbf{F} \quad (1)$$

where $\mathbf{q}$ and $\mathbf{F}$ denote the conductive and radiative heat flux vectors, respectively. The divergence of the radiative flux, $\nabla\cdot\mathbf{F}$, is defined by

$$\nabla\cdot\mathbf{F} = \int_0^\infty \nabla\cdot\mathbf{F}_\lambda\,\mathrm{d}\lambda = \int_0^\infty \kappa_\lambda[4\pi n_\lambda^2 I_{b\lambda}(T) - G_\lambda]\,\mathrm{d}\lambda. \quad (2)$$

The spectral radiative flux vector $\mathbf{F}_\lambda$ and the spectral irradiance G_λ are defined as

$$\mathbf{F}_\lambda = \int_{\Omega=4\pi} I_\lambda(\mathbf{r},\boldsymbol{\Omega})\boldsymbol{\Omega}\,\mathrm{d}\Omega \quad (3)$$

and

$$G_\lambda = \int_{\Omega=4\pi} I_\lambda(\mathbf{r},\boldsymbol{\Omega})\,\mathrm{d}\Omega \quad (4)$$

respectively. In these equations $I_\lambda(\mathbf{r},\boldsymbol{\Omega})$ denotes the spectral radiant intensity which is a function of the direction vector at the spatial position vector $\mathbf{r}$. The divergence of the radiative flux vector $\mathbf{F}$ defined in equation (2) is obtained by solving the radiative transfer equation (RTE) within the semitransparent (absorbing and emitting) medium [9].

The solution of the thermal energy equation, equation (1), requires the specification of an initial temperature distribution and the boundary conditions at each interface of the semitransparent medium. Initially, the semitransparent medium is at uniform temperature T_0, and the initial condition is

$$T(r,z,t) = T_0 \quad \text{at } t = 0. \quad (5)$$

The boundary conditions are obtained from energy balances at each interface. The interface energy balance provides the following relation for the boundary conditions:

$$-k\left.\frac{\mathrm{d}T}{\mathrm{d}n}\right|_s = h(T_s - T_\infty) + \pi\varepsilon[g(T_s)I_b(T_s) - g(T_{sur})I_b(T_{sur})] \quad (6)$$

where n denotes the coordinate normal to the surface such as r and z, and $g(T)$ denotes the fractional blackbody function in the opaque spectral range and is defined as

$$g(T) = \left(\int_0^\infty I_{b\lambda}(T)\,\mathrm{d}\lambda - \int_0^{\lambda_c} I_{b\lambda}(T)\,\mathrm{d}\lambda\right)\Big/\int_0^\infty I_{b\lambda}(T)\,\mathrm{d}\lambda. \quad (7)$$

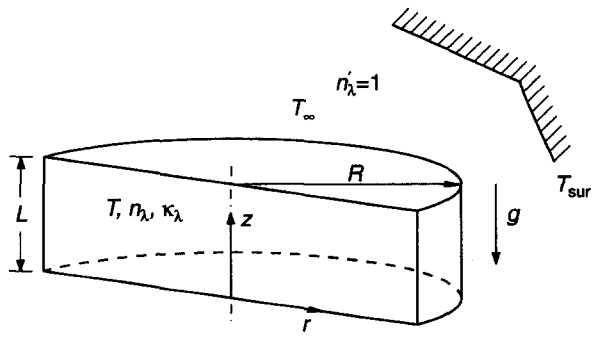

Fig. 1. Schematic of the physical model and coordinate system.

The cut-off wavelength λ_c indicates the wavelength for which the medium is considered to be opaque to radiation. The emissivity ε is for the spectral range where the medium is considered to be opaque.

Radiative transfer model

The radiative transfer equation (RTE) for a spectrally absorbing–emitting medium can be written as [10]

$$(\boldsymbol{\Omega}\cdot\nabla)I_\lambda(\mathbf{r},\boldsymbol{\Omega}) = \kappa_\lambda[n_\lambda^2 I_{b\lambda}(T) - I_\lambda(\mathbf{r},\boldsymbol{\Omega})] \quad (8)$$

where $I_\lambda(\mathbf{r},\boldsymbol{\Omega})$ is the spectral intensity of radiation; $I_{b\lambda}(T)$ is the spectral intensity of blackbody radiation given by Planck's function.

The radiative transfer equation, equation (8), for the spectrally emitting and absorbing axisymmetric medium along a specified discrete direction $\Omega^{m,l}(\theta^m, \phi^l)$ can be expressed as

$$\frac{\mu^{m,l}}{r}\frac{\partial(rI_\lambda^{m,l})}{\partial r} - \frac{1}{r}\frac{\partial(\eta^{m,l}I_\lambda^{m,l})}{\partial\phi} + \xi^{m,l}\frac{\partial I_\lambda^{m,l}}{\partial z} = \kappa_\lambda^{m,l}[n_\lambda^2 I_{b\lambda}(T) - I_\lambda^{m,l}]. \quad (9)$$

In the above equation, ϕ is the azimuthal angle for the direction $\Omega^{m,l}$ relative to the local radial direction, and $\mu^{m,l}$, $\eta^{m,l}$ and $\xi^{m,l}$ are direction cosines and defined by

$$\mu = \sin\theta\cos\phi, \quad \eta = \sin\theta\sin\phi, \quad \xi = \cos\theta. \quad (10)$$

The boundary condition for equation (8) at an optically smooth bounding surface from the interface conditions between the medium and the bounding entity is written as

$$I_\lambda(\mathbf{r},\boldsymbol{\Omega}) = [1-\rho_\lambda(\theta)](n_\lambda/n'_\lambda)^2 I_{b\lambda}(T_{sur}) + \rho_\lambda(\theta)I_\lambda(\mathbf{r},\boldsymbol{\Omega}') \quad \text{for } \boldsymbol{\Omega}\cdot\mathbf{n} > 0 \quad (11)$$

where $\theta = \cos^{-1}(\boldsymbol{\Omega}\cdot\mathbf{n})$

The interaction of radiation at the smooth interface between two dielectric media is governed by Snell's law and Fresnel's equation [10]. The directional reflectivity $\rho_\lambda(\theta)$ of the interface between two dielectric media of different reflective indices is obtained by combing Fresnel's equation for reflection and Snell's law for refraction [9].

Thermophysical and radiative properties of optical quality glass

As an example, cooling of BK7 glass by combined conduction and radiation is considered. The glass is of optical quality and is sodium rich, and has excellent transmission characteristics in the visible and near infrared, making it a popular glass for optical systems. In order to accurately predict the temperature distribution in the glass disk, the specification of thermophysical and radiative properties is needed. All of these properties are given by the manufacturer† and the dependence of the properties with temperature is neglected. Thermophysical properties are assumed to be independent of temperature and are as follows:

Density:	$\rho = 2514.8\ \text{kg m}^{-3}$
Thermal conductivity:	$k = 1.672\ \text{W m K}^{-1}$
Specific heat:	$c = 1239.6\ \text{J kg K}^{-1}$.

The refractive index of BK7 glass given by manufacturer† is expressed as a function of wavelength by Sellmeier dispersion formula:

$$n_\lambda = \sqrt{1 + \frac{B_1\lambda^2}{\lambda^2 - C_1} + \frac{B_2\lambda^2}{\lambda^2 - C_2} + \frac{B_3\lambda^2}{\lambda^2 - C_3}} \quad (12)$$

where the wavelength is in μm and

$$B_1 = 1.03961212, \quad C_1 = 6.00069867\times10^{-3}$$

$$B_2 = 2.31792344\times10^{-4}, \quad C_2 = 2.00197144\times10^{-2}$$

$$B_3 = 1.01046945, \quad C_3 = 1.03560653\times10^{2}.$$

As shown in Fig. 2, the refractive index decreases with wavelength. The absorption coefficient is relatively small in the visible and near infrared parts of the spectrum. BK7 optical glass has good transmission in this spectral region. The glass is considered to be opaque to radiation for wavelengths larger than cut-off wavelength λ_c, which is assumed to be 5 μm. The emissivity in the opaque spectral region ($\lambda \geqslant \lambda_c$) is $\varepsilon = 0.9$.

Method of solution

Since the energy equation is very complex and nonlinear when radiative transfer has been included, the solution is obtained numerically. The finite volume method is used to solve the thermal energy equation, and discrete ordinates method [9] is used to solve the radiative transfer equation in an axisymmetric cylindrical geometry.

Closed form analytical solution of the RTE, equation (8), is not possible because the boundary conditions are complicated functions of direction and wavelength; thus, the discrete ordinates method (DOM) is used to obtain a numerical solution. The accuracy of the method depends on the choice of the quadrature set. Although the choice is arbitrary, a completely symmetric quadrature is preferred in order to preserve geometric invariance of the solution [11]. Moreover, the directional dependence of specularly reflecting boundaries is affected by the choice of the quadrature set to be used, because a weight represents the part of area on a unit sphere for each ordinate direction, and the average value of reflectivity within the range of a weight varies with the type of the quadrature set. Thus, the dependence of reflectivity on quadrature sets was examined [9], and level symmetric

† Schott Glaswerke, Mainz, Germany.

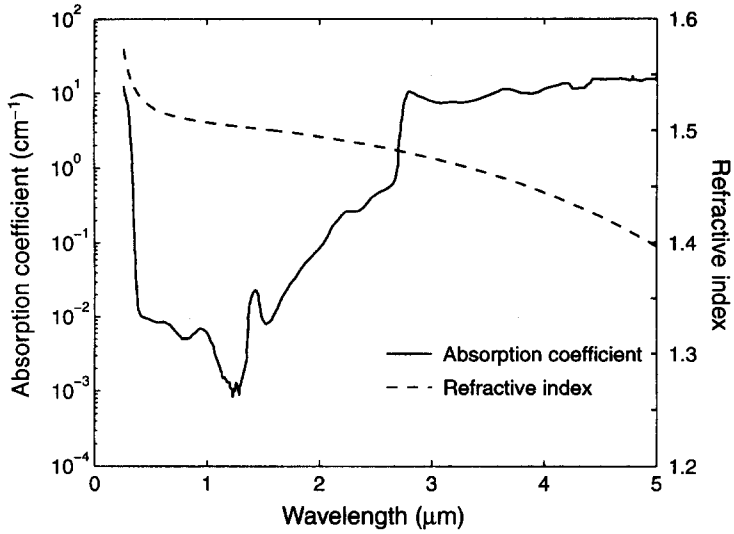

Fig. 2. Spectral absorption coefficient and refractive index of BK7 glass.

higher-order (LSH) quadrature proposed by Fiveland [12] is used in the present analysis.

While implementing the discrete ordinates approximation for the cylindrical geometry, it has been a common practice to assume a uniform distribution of the weighting factor over the calculation domain, regardless of the control volume size [10]. When the uniform weighting factors are used, the numerical predictions often exhibit physically unrealistic negative intensities, and then the numerical treatment to obtain positive intensities is needed. In the present study, an exponential-type scheme proposed by Song and Viskanta [13] is used in order to obtain positive radiative intensity predictions. Details concerning the solution method using discrete ordinates method can be found elsewhere [9] and need not be repeated here.

An implicit time-marching technique is used to calculate the transient variation of temperature. Moreover, the nonlinearity of radiative transfer requires an 'internal integration' to be performed at each time interval to produce consistency between the temperature profile and the radiation field. The internal iterative calculation procedure is shown in Fig. 3. When the implicit time-marching technique is used, the temperature at each node is implicitly updated over a time interval. However, the radiative flux is calculated using the temperatures at the previous time step. Due to the nonlinearity of the energy equation with temperature the radiative flux needs to be updated with the temperature at the current time step. Of course, if very fine time interval ($\Delta t \geqslant 0.1$ s in the present study) is used, the internal iteration may not be needed. If internal iteration is used, accurate temperature predictions can be obtained with a relatively large time interval.

Figure 4 shows the transient temperature variations by marching in time. The time step used in the present study varies with time and is given as follows:

$\Delta t = 0.01$ s for $0 \leqslant t < 0.1$ s

$\Delta t = 0.1$ s for $0.1 \leqslant t < 1$ s

$\Delta t = 1$ s for $1 \leqslant t < 300$ s

$\Delta t = 5$ s for $300 \leqslant t < 1200$ s

$\Delta t = 10$ s for $1200 \leqslant t < 2400$ s

$\Delta t = 20$ s for $2400 \leqslant t < 3600$ s

$\Delta t = 30$ s for $3600 \leqslant t < 7200$ s

$\Delta t = 60$ s for $t \geqslant 7200$ s.

In Fig. 4, the transient temperature variations are predicted up to $t = 100$ s. For $\Delta t \leqslant 0.1$ s, the internal iteration is not needed in the problem considered. The temperature variations obtained with the variable time step are in good agreement with the temperature variations without internal iteration for $\Delta t = 0.1$ s. Since the variable time step is $\Delta t = 1$ s for $1 \leqslant t < 300$ s, the temperature variation obtained with the time step can be compared to that with $\Delta t = 1$ s and without internal iteration. The temperature with $\Delta t = 1$ s and without internal iteration overpredicts the temperature with internal iteration. When the time step becomes larger such as $\Delta t = 5$ s, the overprediction also becomes larger due to the nonlinear dependence of radiative transfer on temperature. However, if the internal iteration is used together with large time step such as $\Delta t = 5$ s, accurate results can be obtained. The internal iteration for $\Delta t = 1$ s converges in three iterations to within the accuracy of 1×10^{-5}. Thus, the computer time requirement is reduced by 70% when compared to that required to obtain the result without internal iteration and with $\Delta t = 0.1$ s.

The sensitivity of solution to the choice of the grid system was carried out as shown in Fig. 5. The grid spacing used is not uniform, but is more compact near

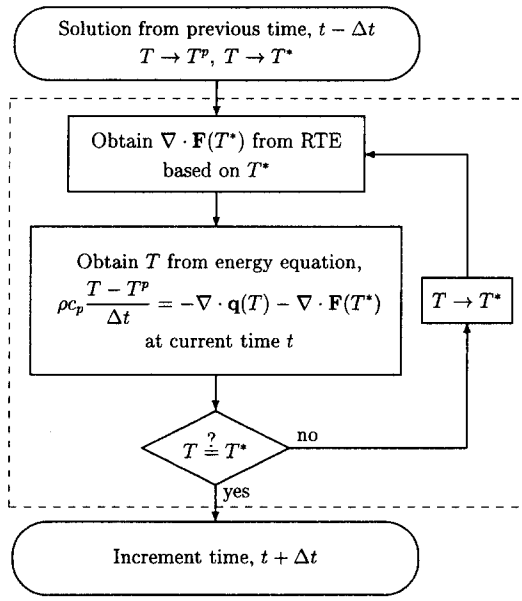

Fig. 3. Schematic of internal iterative calculation procedure.

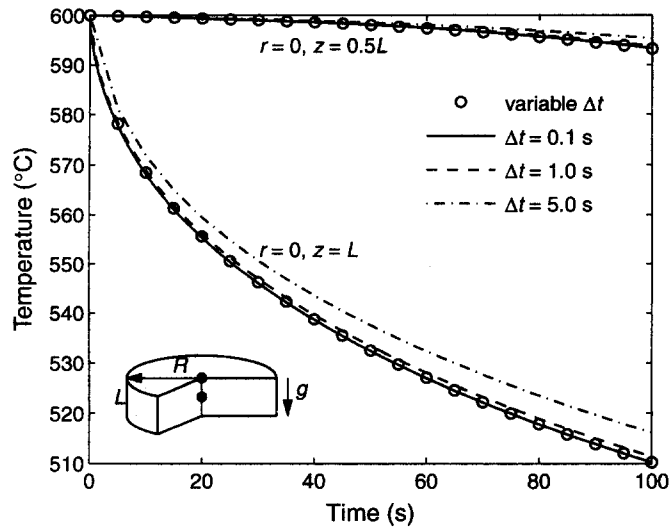

Fig. 4. Transient temperature variation with marching time increment.

the axis of symmetry and the bounding interfaces. This was done in order to resolve the steep spatial changes in the physical variables expected in these regions. The results obtained using 61×31 grid are in good agreement with that using 81×41. The 61×31 grid is used in the numerical results reported in the paper. The sensitivity test for the number of spectral bands was performed, and eight spectral bands are used in the present analysis, since the results with eight bands were sufficiently accurate compared to the results obtained with larger than 24 bands [9].

RESULTS AND DISCUSSION

Model validation

One-dimensional solution is first obtained for the purpose of comparing the numerical predictions to the available experimental data [3]. A comparison for a two-dimensional axisymmetrical geometry would have been highly desirable, but neither experimental data nor numerical results which are appropriate for the purpose of the present study are available. Thus, the boundary conditions have been modified to obtain

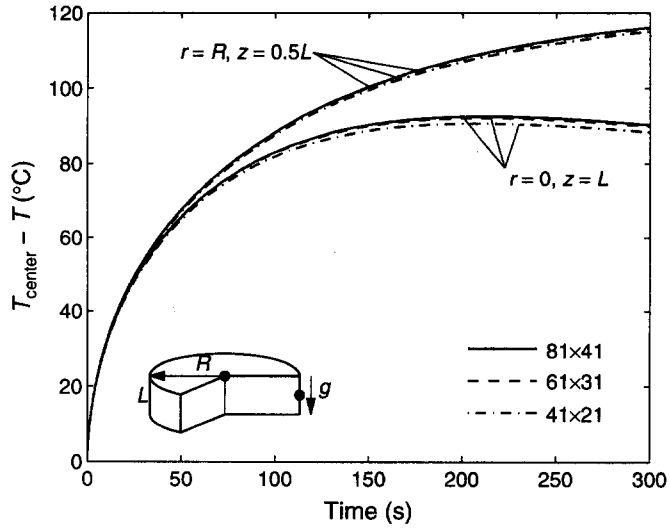

Fig. 5. Effect of grid size on the transient temperature variations.

a one-dimensional solution from the two-dimensional formulation. The reflectivity at the circumference ($r = R$) of the glass disk was assumed to be unity for the entire range of incident angles of the intensity, and the boundary condition at the surface for conductive transfer was assumed to be adiabatic. Since the experimental data [3] is for a 11.68 mm thick soda-lime glass plate, the thermophysical and radiative properties of soda-lime glass are taken from those used in the analysis of Field and Viskanta [3], excluding thermal conductivity, which is given by an empirical relation by Mann *et al.* [14]. Five spectral bands are used for the radiative transfer calculations, and the natural convection heat transfer coefficient is taken to be $h = 4.25$ W m^{-2} K^{-1}.

The comparisons are shown in Figs. 6 and 7. Figure 6 shows that the predictions are in good agreement with the experimental data if the uncertainty of experimental data and thermophysical properties, especially the specific heat, is considered. The difference between the predicted temperature and the experimental data at $t = 450$ s is less than 6%, and is within the experimental uncertainty [3]. There is uncertainty in the specific heats reported in the literature [14], and the specific heat-temperature relations vary from 100 to 125 J kg K^{-1} in the temperature range considered here. If a smaller specific heat is used, the transient temperature shown in Fig. 6 would also be closer to the experimental data. Figure 7 shows the temperature difference between the center and the surface as a function of time. This is a very critical comparison between predictions and data. The figure reveals the

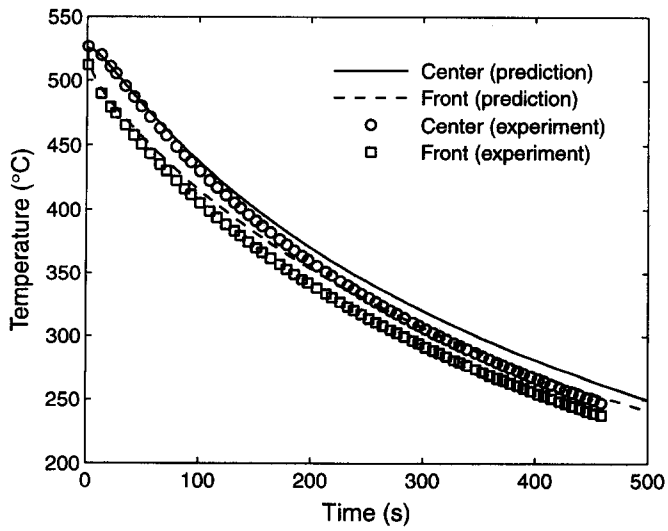

Fig. 6. Comparison of predicted transient temperature variations with experimental data of Field and Viskanta [3] for an 11.68 mm thick soda-lime glass plate.

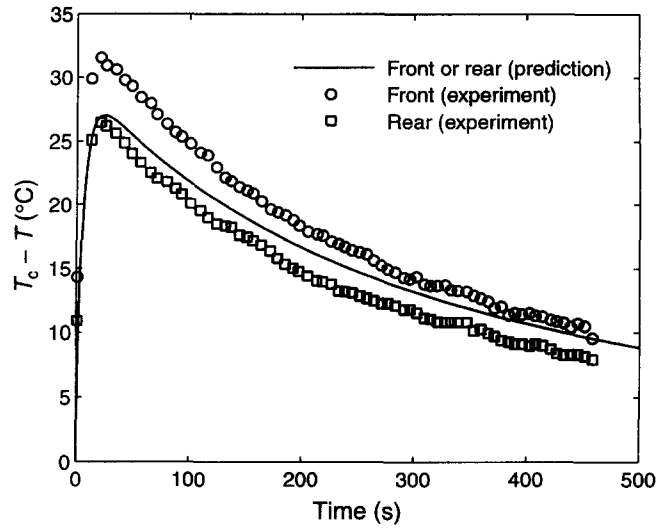

Fig. 7. Comparison of predicted temperature difference with experimental data of Field and Viskanta [3] for an 11.68 mm thick soda-lime glass plate.

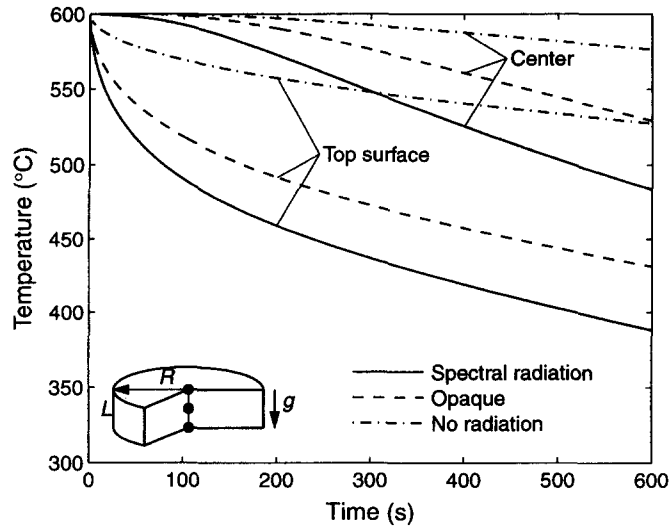

Fig. 8. Effect of radiation on the transient temperature variations for constant free convection heat transfer coefficients.

front and rear surface temperatures measured in the experiment are not the same, and this suggests that the cooling in the experiments was not symmetric. The numerical solution falls between the variations in temperature differences at two surfaces, and the maximum temperature difference occurs at $t = 24$ s. The measured maximum temperature difference occurs at $t = 20.9$ s.

Conductive–radiative cooling of a BK7 glass disk

The results for conductive–radiative cooling of a BK7 optical quality glass disk are given in Figs. 8–15. The dimensions of the disk considered here and the temperature conditions for cooling are as follows:

Radius:	$R = 100$ mm
Thickness:	$L = 50$ mm
Initial temperature:	$T_0 = 600$°C
Surroundings temperature:	$T_{sur} = 20$°C
Ambient temperature:	$T_\infty = 20$°C.

In addition, three types of ambient conditions for cooling the glass disk are considered as:

Radiation only:	$h = 0$
Free convection and radiation:	$h =$ constant
Free convection and radiation:	$h = h(T)$.

When $h = 0$ (vacuum), the thermal energy from the hot glass disk is transferred to the surroundings by

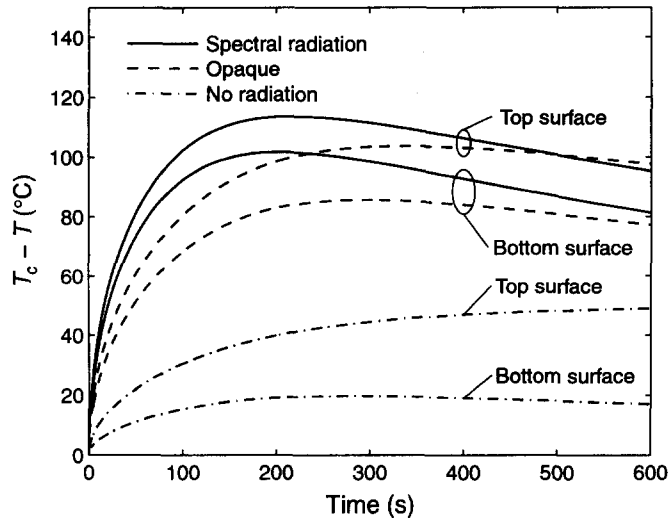

Fig. 9. Effect of radiation on the temperature difference variations for constant free convection heat transfer coefficients.

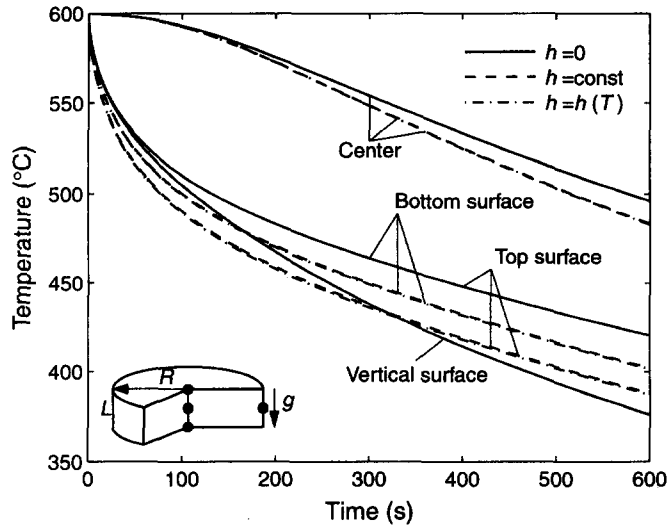

Fig. 10. Effect of ambient conditions on the transient temperature variations.

radiation only. However, when the ambient atmosphere is not vacuum, the hot glass disk is cooled by both free convection and thermal radiation. Then, the convection heat transfer coefficient has to be specified. The correlations for external free convection over isothermal surfaces [15] are used in the present analysis to determine the average heat transfer coefficients at each face of the disk. The Rayleigh numbers for the temperature conditions considered here are in the range of $10^4 < Ra < 10^8$. In order to investigate the effect of heat transfer coefficient on the cooling of the glass disk, two types of heat transfer coefficients such as h = constant and $h = h(T)$ are determined. The average heat transfer coefficient $h(T)$ is estimated from the empirical correlations [15] accounting for the temperature dependent thermophysical properties of air at each surface. The constant heat transfer coefficients are average values over the temperature range of $200 < T < 600$°C, obtained by using the same relation, $h = h(T)$, and are 11.2, 5.6 and 10.7 W m^2 K^{-1} in the top, bottom and vertical faces, respectively.

Temperature distribution

Figure 8 shows the effect of radiation on the transient temperature variations for h = constant. When radiation is not considered, the glass disk is cooled slowly and the temperature differences between the surface and the center are relatively small. However, it is clear in Fig. 9 that the temperature difference between the top surface and the center is much larger than that between the bottom surface and the center,

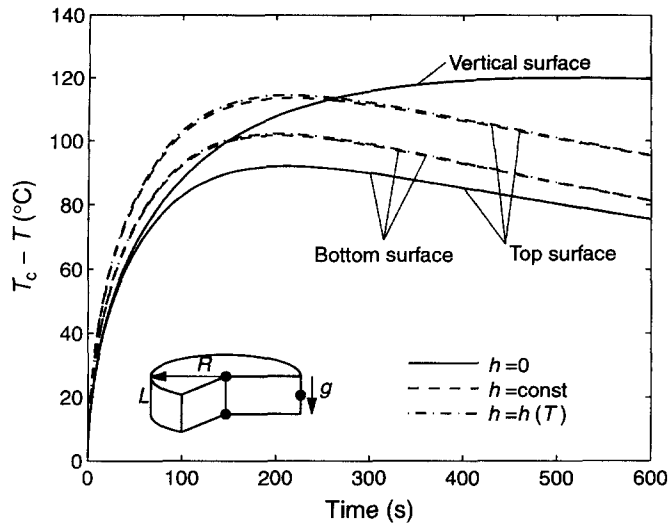

Fig. 11. Effect of ambient conditions on the temperature difference variations.

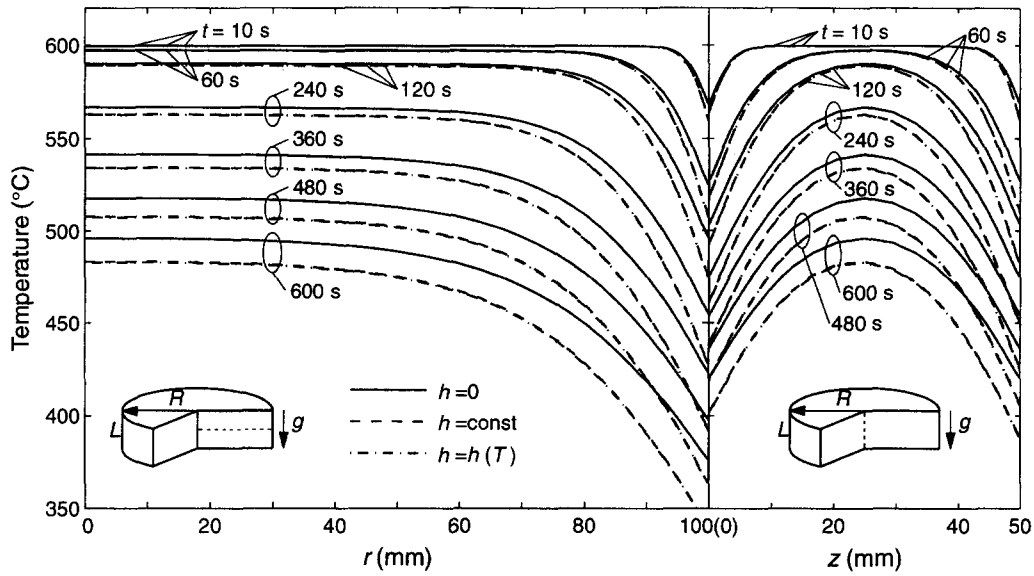

Fig. 12. Center line and midplane temperature distributions with time.

and a symmetric temperature distribution cannot be expected. This is an unrealistic prediction because radiation should be included. If the glass is considered to be opaque to radiation, the disk is cooled more rapidly, and the maximum temperature difference occurs at $t \approx 300$ s. The surface emissivity is assumed to be 0.9. As a first approximation, glass can be assumed to be opaque, because the analysis of spectral radiative transfer is complex. However, when the glass is assumed to be opaque to radiation the cooling of the glass disk is much slower than when it is semitransparent to radiation even though the surface emissivity (or absorptivity) is relatively large ($\varepsilon = 0.9$). Thus, the use of the approximation is not recommended.

In a semitransparent material such as glass, thermal energy is redistributed within the glass by radiation and is transferred from the interior of the glass to surroundings by 'long range' radiative transfer. Thus, the analysis based on the opaque model cannot predict the local heat transfer rate correctly. The glass is cooled rapidly when spectral radiation is considered (Fig. 8), and the maximum temperature difference between the surfaces and the center occur at $t \approx 200$ s (Fig. 9). Even though the maximum temperature differences between the surfaces and the center are larger than those based on the opaque model, the temperature differences decrease with time and finally become smaller than those predicted for the opaque model. Moreover, since the temperature difference

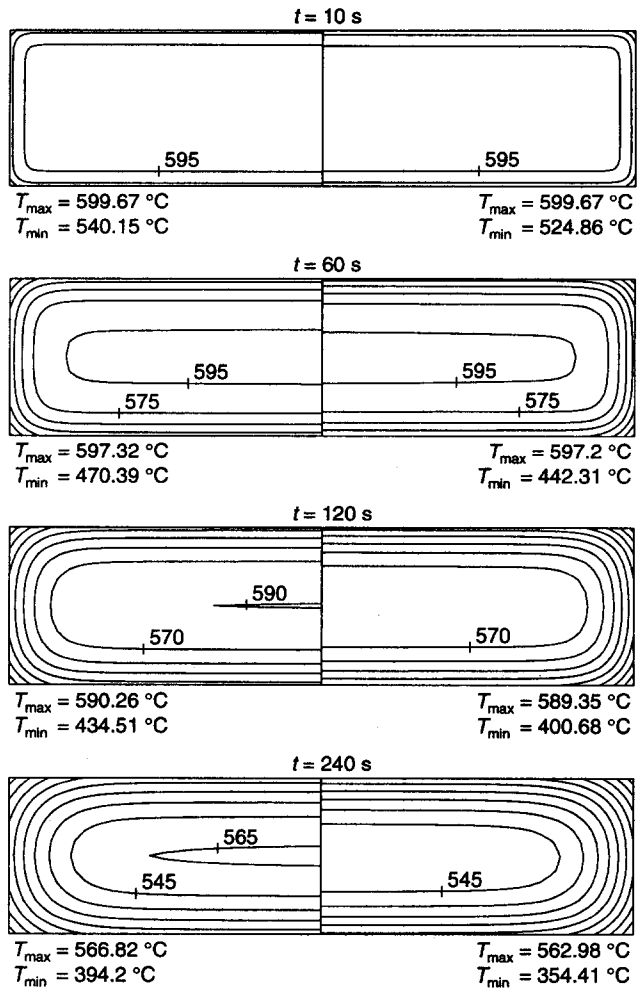

Fig. 13. Comparison of temperature isopleths for different cooling conditions: left panels for $h = 0$ and right panels for $h = \text{const}$.

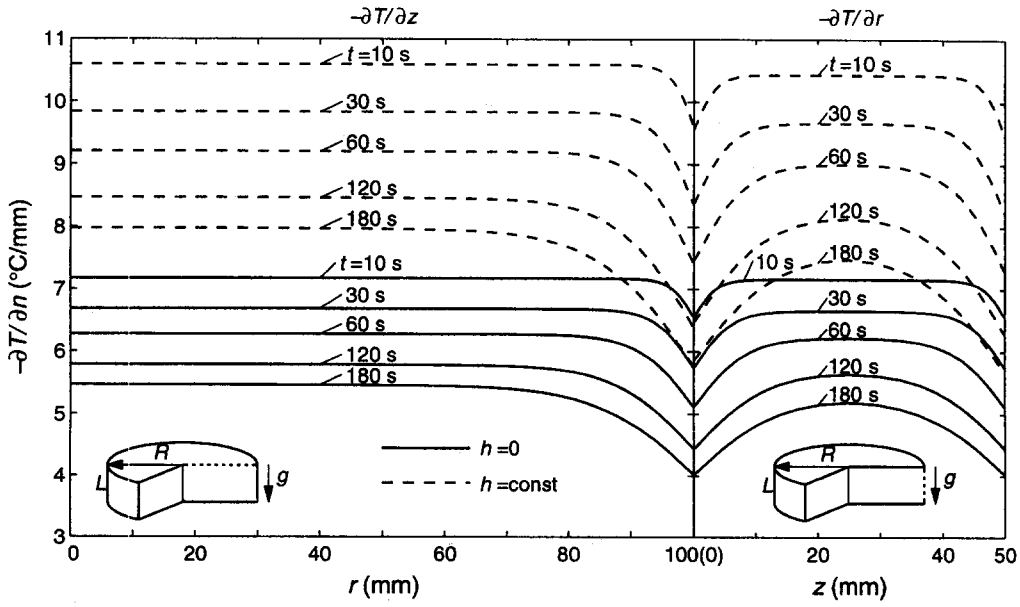

Fig. 14. Effect of convective heat transfer on the surface temperature gradients.

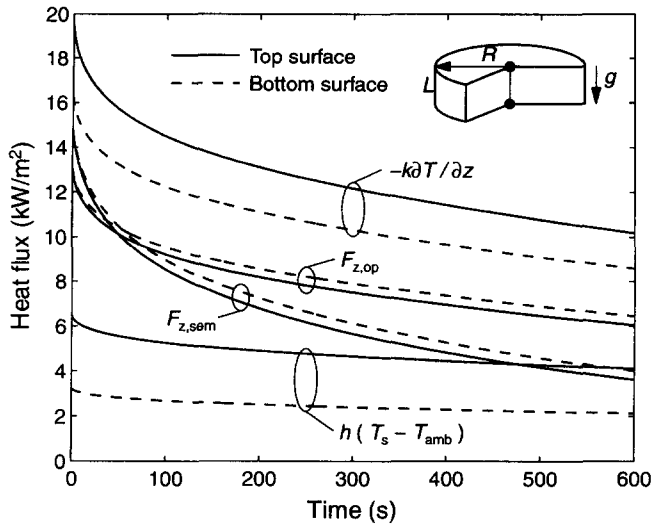

Fig. 15. Transient surface heat flux variations for h = const.

between the top surface and the bottom surface is relatively small, the degree of asymmetry in the temperature distribution within the glass disk caused by free convection is also not large. This means that thermal energy is effectively redistributed by radiation within the glass disk. The finding is apparent by comparing the results with those for the case in the absence of radiation.

Figures 10 and 11 show the effect of ambient conditions on the transient temperature variations. As mentioned above, the results obtained with three types of ambient conditions are compared in the figures. Figure 10 shows the transient temperature variations at the center and surfaces of the glass disk. When the ambient surroundings are assumed to be vacuum ($h = 0$), the hot glass disk is cooled only by radiation, and the temperature distribution is symmetric about the center plane ($z = 0.5L$) as noted in Figs. 12 and 13. Under free convection conditions, the symmetric temperature distribution cannot be preserved, because the heat transfer coefficients, are different at the top and bottom faces. The average heat transfer coefficient at the top surface is about two times greater than that at the bottom surface. However, since the fraction of cooling by radiation is much larger than that by free convection and the thermal energy is redistributed by radiation within the glass disk, the degree of asymmetry is greatly reduced when compared to the cooling in the absence of radiation. The glass disk is cooled more rapidly when free convection and radiation are considered. In the case of h = constant, temperature at the center ($r = 0, z = 0.5L$) decreases by 3.1°C at $t = 211$ s, and temperatures at the top ($r = 0, z = L$) and bottom surfaces ($r = 0, z = 0$) decrease by 24 and 12.6°C, respectively, when compared to the case with $h = 0$.

Figure 11 shows the temperature differences between the top ($r = 0, z = L$) or bottom surfaces ($r = 0, z = 0$) and the center ($r = 0, z = 0.5L$) with time. Since the temperature difference between the surface and the center is usually used as a first approximation for the rate of cooling, it is interesting to compare the maximum temperature difference. The differences between the top or bottom surfaces and the center occur at about 200 s. When $h = 0$, the maximum temperature difference between the surface and the center is 91.12°C at $t = 211$ s, whereas when h = constant, the maximum temperature difference is 113.6°C at $t = 217$ s at the top surface and 101.7°C at $t = 202$ s at the bottom surface. Thus, when free convection is considered, the maximum temperature difference is larger than that when only radiation is accounted for, and the glass disk is cooled more rapidly.

Figure 12 shows the temperature distributions along the center lines in the r- and z-directions. The temperature distribution in the glass disk becomes nonuniform very rapidly. After 10 s, the temperature in the radial direction is nearly uniform within the glass, except in the immediate vicinity of the boundaries. At $t = 60$ s, the temperature distribution in the radial direction is nearly uniform except in the vicinity of the circumference, but the distribution in the axial direction has become less uniform. Moreover, when the glass is cooled by free convection and radiation, the temperature distribution in the axial direction becomes non-symmetric. This is clearly evident from the results given in Fig. 13, which shows the isotherms in the glass disk at different times for two different ambient cooling conditions.

Heat transfer

Figure 14 shows the temperature gradients at the top and vertical surfaces. When free convection and radiation occur simultaneously, the temperature gradients are about a factor of 1.5 greater than when

heat transfer from the disk is only by radiation. The gradients are relatively uniform over the edge of the disk, except in the vicinity of the edge of the disk (at $r = R$ and $z = 0$ or $z = L$). The temperature gradients are smaller at the edge than at the face owing to the strongly two-dimensional nature of heat transfer by conduction and radiation in this region of the glass disk.

Figure 15 illustrates the transient temperature variations at two selected locations for h = constant. The temperature gradients at the surfaces decrease rapidly during the early times (< 100 s) and then the decrease is much slower. The cooling rate by free convection is smaller than by radiation, and the heat flux by free convection also decrease more slowly than by radiation. At early times, the radiative cooling predominates over the cooling by free convection. The latter becomes dominant at later times after the temperature has decreased.

The cooling by radiation can be easily explained by dividing the spectrum into semitransparent and opaque wavelength regions. Initially, the radiative flux is larger in the semitransparent spectral region than in the opaque region. When temperature is high, the fraction of the radiation emitted in the semitransparent region ($0 \leqslant \lambda < \lambda_c$) is greater than in the opaque region ($\lambda_c \leqslant \lambda < \infty$). As the temperature decreases, a larger fraction of radiation is emitted in the opaque spectral region [9]. Thus, as the temperature of the disk decreases, the fraction of radiative cooling in the opaque region becomes larger than in the semitransparent region (after $t = 49$ s at the top surface and $t = 54$ s at the bottom surface). Figure 15 also shows that the cooling by free convection causes the temperature distribution within the disk to become nonsymmetric due to the large difference in the convective heat fluxes at the two surface. The heat transfer coefficient at the top surface is greater than at the bottom surface by a factor of about two, and the heat loss by free convection at the top surface is also as much greater than at the bottom surface. However, since the radiative fluxes, $F_{z,\mathrm{sem}}$ and $F_{z,\mathrm{op}}$, at the bottom surface are a little greater than those at the top surface due to higher temperature at the bottom surface, this reduces the degree of asymmetry in the temperature distribution within the disk in the axial direction.

CONCLUSION

The problem of transient heat transfer by combined conduction and radiation in an optical quality glass disk has been solved numerically. The radiative transfer equation for an axisymmetric cylindrical geometry has been solved using the discrete ordinates method, and spectral nature of radiation as well as direction-dependent reflection and transmission across the interfaces have been accounted for. The physical model and the numerical procedure used are validated by comparing the predicted transient temperatures against experimental data for float glass.

Based on the numerical results obtained the following conclusions can be drawn. The results obtained show that the spectral nature of radiation should be considered to accurately predict the temperature distribution in a semitransparent medium such as glass. When the optical quality glass disk is assumed to be opaque to radiation, the predicted temperature variations differ greatly from those obtained on the basis spectral radiative transfer, and the disk is cooled more slowly.

The presence of convection during cooling of glass disks increases the temperature nonuniformity in the glass, particularly near the edge. Since the free convection heat transfer rates at the top and bottom faces of the glass disk are different, the temperature distributions predicted are not symmetric about the midplane; however, radiative transfer reduces the degrees of asymmetry.

Radiation accounts for a large fraction of the total heat transfer rate during the initial cooling phase when temperature is high, and the rapid variation of temperature and temperature gradients is detrimental to achieving the glass disks of high optical quality. The fraction of radiative cooling in the semitransparent part of the spectral is larger than in the opaque region when the temperature of the glass is high. As the temperature decreases, the role of radiation heat transfer from the surface in the opaque spectral region increases. Thus, in order to accurately predict the cooling process of an optical quality glass, analysis of radiative transfer including the spectral dependence of the absorption coefficient on wavelength must be accounted for.

Acknowledgement—The authors wish to express their thanks to Dr Frank-Thomas Lentes of Schott Glaswerke, Mainz, Germany for providing thermophysical and optical property data of BK7 optical glass as well as for information on the annealing process.

REFERENCES

1. Bach, H. and Neuroth, N., eds, *The Properties of Optical Glass*. Springer-Verlag, Berlin, 1995.
2. Gardon, R., A review of radiant heat transfer in glass. *Journal of the American Ceramic Society*, 1961, **44**, 305–312.
3. Field, R. E. and Viskanta, R., Measurement and prediction of the temperature distribution in soda-lime glass plates. *Journal of the American Ceramic Society*, 1990, **73**, 2047–2053.
4. Viskanta, R. and Anderson, E. E., Heat transfer in semitransparent solids. In *Advances in Heat Transfer*, Vol. 11, ed. T. F. Irvine, Jr and J. P. Hartnett. Academic Press, New York, 1975, pp. 318–441.
5. Bergman, T. L. and Viskanta, R., Radiation heat transfer in manufacturing and materials processing. In *Radiative Transfer—I*, ed. M. P. Mengüç. Begell House, New York, 1996, pp. 13–39.
6. Gardon, R., Calculation of temperature distribution in glass plates undergoing heat treatment. *Journal of the American Ceramic Society*, 1958, **44**, 305–312.
7. Ping, T. H. and Lallemand, M., Transient radiative–conductive heat transfer in flat glasses submitted to temperature, flux and mixed boundary conditions. *Inter-*

national Journal of Heat and Mass Transfer, 1989, **32**, 795–810.
8. Su, M.-H. and Sutton, W. H., Transient conductive and radiative heat transfer in a silica window. *Journal of Thermophysics and Heat Transfer*, 1995, **9**, 370–373.
9. Lee, K. H. and Viskanta, R., Prediction of spectral radiative transfer in a condensed cylindrical medium using discrete ordinates method. *Journal of Quantitative Spectroscopy and Radiative Transfer*, 1997, **58**, 329–345.
10. Modest, M. F., *Radiative Heat Transfer*. McGraw-Hill, Highstown, New Jersey, 1993.
11. Lathrop, K. D. and Carlson, B. G., Discrete ordinates angular quadrature of neutron transport equation. Technical Report, LA-3186, Los Alamos Scientific Laboratory, Los Alamos, New Mexico, 1965.
12. Fiveland, W. A., The selection of discrete ordinate quadrature sets for anisotropic scattering. *Fundamentals of Radiation Heat Transfer*, HTD-Vol. 160. ASME, New York, 1991, pp. 89–96.
13. Song, M. and Viskanta, R., Discrete ordinates solution of axisymmetric radiative transfer within a condensed semitransparent medium having specularly reflecting boundaries. In *Proceedings of National Heat Transfer Conference*, HTD-Vol. 325, 3. ASME, New York, 1996, pp. 55–62.
14. Mann, D., Field, R. E. and Viskanta, R., Determination of specific heat and true thermal conductivity of glass from dynamic temperature data. *Wärme- und Stoffübertragung*, 1992, **27**, 225–231.
15. Jaluria, Y., Basics of natural convection. In *Handbook of Single-Phase Convective Heat Transfer*, ed. S. Kakac, R. K. Shah and W. Aung. John Wiley and Sons, New York, 1987.